

Detection of cyclooxygenase-2-derived oxygenation products of the endogenous cannabinoid 2-arachidonoylglycerol in mouse brain

Amanda Morgan, Philip J. Kingsley, Michelle M Mitchener, Megan Altemus,
Toni Patrick, Andrew Gaulden, Lawrence J. Marnett, and Sachin Patel

ACS Chem. Neurosci., **Just Accepted Manuscript** • DOI: 10.1021/acschemneuro.7b00499 • Publication Date (Web): 03 May 2018

Downloaded from <http://pubs.acs.org> on May 4, 2018

Just Accepted

“Just Accepted” manuscripts have been peer-reviewed and accepted for publication. They are posted online prior to technical editing, formatting for publication and author proofing. The American Chemical Society provides “Just Accepted” as a service to the research community to expedite the dissemination of scientific material as soon as possible after acceptance. “Just Accepted” manuscripts appear in full in PDF format accompanied by an HTML abstract. “Just Accepted” manuscripts have been fully peer reviewed, but should not be considered the official version of record. They are citable by the Digital Object Identifier (DOI®). “Just Accepted” is an optional service offered to authors. Therefore, the “Just Accepted” Web site may not include all articles that will be published in the journal. After a manuscript is technically edited and formatted, it will be removed from the “Just Accepted” Web site and published as an ASAP article. Note that technical editing may introduce minor changes to the manuscript text and/or graphics which could affect content, and all legal disclaimers and ethical guidelines that apply to the journal pertain. ACS cannot be held responsible for errors or consequences arising from the use of information contained in these “Just Accepted” manuscripts.



Detection of cyclooxygenase-2-derived oxygenation products of the endogenous cannabinoid 2-arachidonoylglycerol in mouse brain

Amanda Morgan^{1,3}, Phillip J. Kingsley², Michelle M. Mitchener², Megan Altemus¹, Toni Patrick¹, Andrew Gaulden¹, Lawrence J. Marnett², and Sachin Patel^{1,3,4*}

Department of ¹Psychiatry and Behavioral Sciences, ²A.B. Hancock Jr. Memorial Laboratory for Cancer Research, Departments of Biochemistry, Chemistry, and Pharmacology, Vanderbilt Institute of Chemical Biology, ³Department of Molecular Physiology & Biophysics and ⁴The Vanderbilt Brain Institute
Vanderbilt University Medical Center, Nashville, TN 37232

*Correspondence:

Sachin Patel, MD, PhD

Associate Professor

Departments of Psychiatry and Behavioral Sciences,

Molecular Physiology & Biophysics, and

Pharmacology

2213 Garland Avenue

Medical Research Building IV, Rm 8425B

Vanderbilt University Medical Center

Nashville, TN 37232

Email: sachin.patel@vanderbilt.edu

Phone: (615) 936-7768

Fax: (615) 322-1462

Abstract

Cyclooxygenase-2 (COX-2) catalyzes the formation of prostaglandins, which are involved in immune regulation, vascular function, and synaptic signaling. COX-2 also inactivates the endogenous cannabinoid (eCB) 2-arachidonoylglycerol (2-AG) via oxygenation of its arachidonic acid backbone to form a variety of prostaglandin glyceryl esters (PG-Gs). Although this oxygenation reaction is readily observed *in vitro* and in intact cells, detection of COX-2-derived 2-AG oxygenation products has not been previously reported in neuronal tissue. Here we show that 2-AG is metabolized in the brain of transgenic COX-2-overexpressing mice and mice treated with the lipopolysaccharide to form multiple species of PG-Gs that are detectable only when monoacylglycerol lipase is concomitantly blocked. Formation of these PG-Gs is prevented by acute pharmacological inhibition of COX-2. These data provide evidence that neuronal COX-2 is capable of oxygenating 2-AG to form a variety PG-Gs *in vivo* and support further investigation of the physiological functions of PG-Gs.

Keywords

Endocannabinoid, prostaglandin glyceryl esters, cannabinoid, monoacylglycerol lipase,

Lumiracoxib, lipopolysaccharide, prostamide

Introduction

Endogenous cannabinoids (eCBs) are a class of bioactive lipid signaling molecules implicated in a variety of physiological processes including appetite regulation, energy homeostasis, cardiovascular function, motivation, anxiety, and sleep¹⁻⁵. Within neurons, the eCBs 2-AG and anandamide (AEA) are generated in an activity-dependent manner and serve primarily as retrograde signaling molecules that reduce presynaptic neurotransmitter release via activation of type-1 cannabinoid receptors⁶. eCBs may also have direct postsynaptic effects on membrane potential and neuronal excitability^{7, 8}. Despite these well-established roles of eCBs, how these lipids are metabolized via non-canonical routes to generate potentially distinct signaling molecules is an active area of investigation.

The exact biosynthesis of AEA is poorly understood, but AEA is primarily metabolized by neuronal fatty-acid amide hydrolase (FAAH) to arachidonic acid (AA)⁹. However, COX-2 can also metabolize AEA to form prostaglandin ethanolamides (PG-EAs; prostamides)¹⁰. The prostamides include PGE₂-EA, PGD₂-EA, and PGF_{2 α} -EA and have been previously detected *in vivo*, supporting the notion that COX-2 serves as a non-canonical eCB metabolic enzyme. For example, PGF_{2 α} -EA is detected upon COX-2 upregulation in both rodent dorsal spinal neurons after carrageenan-induced knee inflammation¹¹ and in preadipocyte cells where PGF_{2 α} -EA acts to prevent adipogenesis¹². It has been suggested that the ability to detect prostamides *in vivo* may be facilitated by their relative metabolic stability and lack of metabolism by FAAH¹³.

2-AG is a highly abundant eCB that mediates retrograde inhibition at central glutamatergic and GABAergic synapses¹⁴. Synaptic 2-AG is generated via the sequential actions of phospholipase C and diacylglycerol lipase- α , in response to a variety of activity-dependent mechanisms. In addition to its signaling functions, 2-AG is thought to be the most common

1
2
3 source of AA for PG production in the CNS¹⁵. The synaptic actions of 2-AG are terminated
4
5 predominantly via monoacylglycerol lipase (MAGL), but also by α/β -hydrolase domain 6 and
6
7 12, as well as COX-2¹⁶. Indeed, 2-AG is efficiently oxygenated by COX-2 *in vitro* to form
8
9 prostaglandin glyceryl esters (PG-Gs), and 2-AG-mediated retrograde synaptic inhibition can be
10
11 enhanced by pharmacological inhibition of COX-2^{10, 17-20}. Despite being detected in
12
13 macrophages following lipopolysaccharide (LPS) administration²¹⁻²³ and in inflamed rat
14
15 hindpaw²⁴, COX-2-derived oxidative metabolites of 2-AG in brain have remained elusive. It is
16
17 possible that PG-Gs are hydrolytically unstable *in vivo* or rapidly further metabolized, and thus
18
19 have eluded detection. Given that PG-Gs have been recently identified as endogenous agonists of
20
21 P2Y6 receptors²⁵ and implicated as neuronal signaling molecules¹⁶ and pain modulators in the
22
23 periphery²⁴, a clearer understanding of the conditions under which PG-Gs are formed is needed.

24
25
26 Here we use an LPS model of neuroinflammation, a transgenic COX-2 overexpression
27
28 model, and pharmacological approaches combined with stable isotope-dilution liquid
29
30 chromatography-tandem mass spectrometry (LC-MS/MS) to detect and quantify PG-G formation
31
32 in mouse brain for the first time. These data provide evidence that neuronal COX-2 can produce
33
34 PG-Gs in the brain when 2-AG levels are elevated via MAGL inhibition and provide direct
35
36 support for the contention that neuronal COX-2 metabolizes 2-AG *in vivo*.

37 38 39 40 41 42 43 44 45 **Results and Discussion**

46
47 We first optimized our analytical detection of PG-Gs by LC/MS/MS using deuterated
48
49 PGE₂-G and PGD₂-G as authentic standards. PGE₂-G, PGD₂-G and PGF_{2 α} -G were identified and
50
51 quantified by LC-MS/MS analysis. These three analytes and the internal standards (PGE₂-G-d5
52
53 and PGF_{2 α} -G-d5) were ionized by complexation with the ammonium cation, resulting in an
54
55
56
57
58
59
60

1
2
3 [M+NH₄]⁺ complex. Multiple product ions were observed when this complex was subjected to
4 collision induced dissociation (CID). For example, the CID spectrum of the [PGE₂-G+NH₄]⁺
5 complex (*m/z* = 444.3) is shown in Fig. 1a, where the product ions at *m/z* 391.2, 317.3, and 299.0
6 are observed. Fragmentation of the [PGD₂-G+NH₄]⁺ complex gives a similar spectrum (not
7 shown). For both PGE₂-G and PGD₂-G, the selected reaction monitoring (SRM) transition *m/z*
8 444.2 – 391.1 was used for quantitative analysis as this transition gave the greatest signal:noise
9 ratio. Table S1 gives the SRM transitions for all analytes reported here. The chromatographic
10 system we employed here was able to resolve the *sn*-1 and *sn*-2 isomers of PGE₂-G, PGD₂-G and
11 PGF_{2α}-G (Fig. S1). PG-Gs are monoacylglycerols and thus will undergo isomerization from the
12 presumed original *sn*-2 conformation to the thermodynamically favored *sn*-1 conformation.
13 Importantly, LC-MS/MS analysis using alternative SRM transitions (*m/z* 444.2 – 317.1 & 444.2
14 – 299.0) generated nearly identical chromatograms to that generated by *m/z* 444.2 – 391.1
15 transition, providing compelling support for our accurate and reliable detection of authentic PG-
16 Gs using our analytical approach (Fig. S2 a-b).
17
18
19
20
21
22
23
24
25
26
27
28
29
30
31
32
33
34
35
36
37
38
39
40
41
42
43
44
45
46
47
48
49
50
51
52
53
54
55
56
57
58
59
60

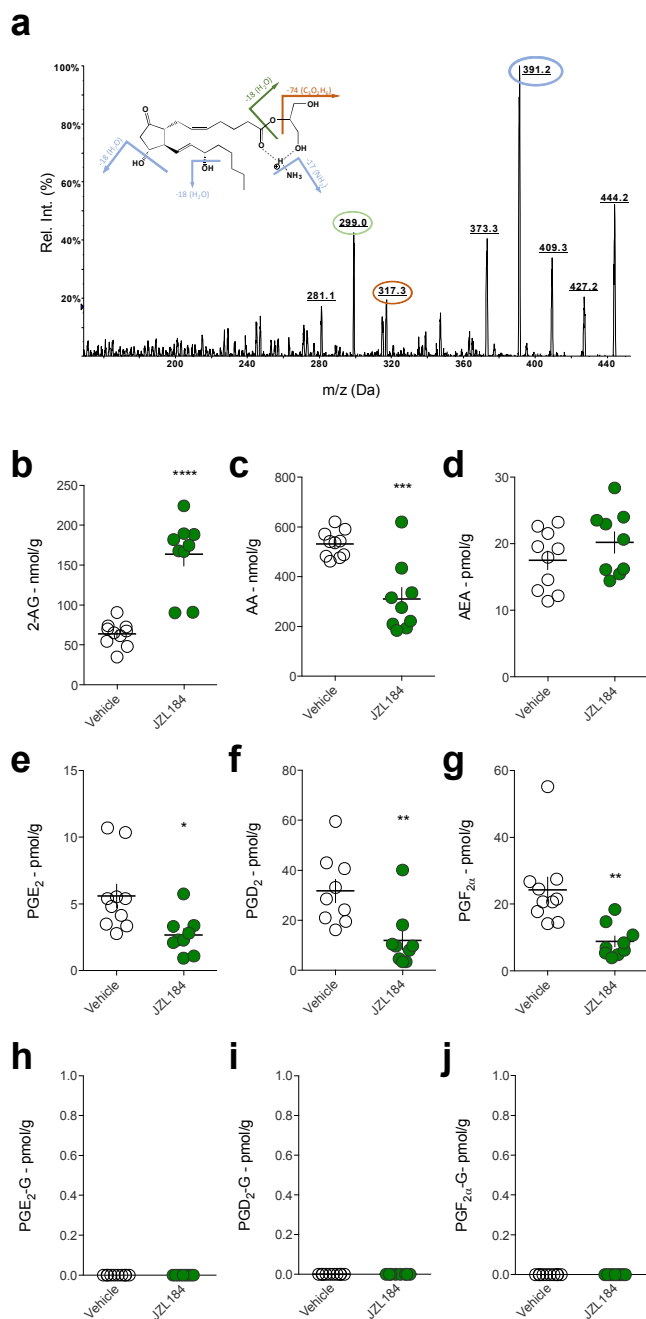


Figure 1. PG-Gs are not detected in C57/Bl6J mouse brain after MAGL inhibition. (a) CID spectra of PGE₂-G. Upon CID, the ammonium complex of PGE₂-G (*m/z* 444) undergoes sequential loss of NH₃ and two molecules of H₂O to generate the product ions at *m/z* 427, 409 and 391, respectively. Subsequently, *m/z* 391 species will undergo a loss of H₂O and C₃H₆O₂ (74 Da) – in either order – to generate the product ions at *m/z* 373, 317 and 299. Circled peak 391 was used for quantitative analysis while 299 and 317 were used for confirmatory analysis (see Fig. S1). (b-d) Effects of JZL184 on 2-AG, AA, and AEA levels in mouse brain. (e-g) Effects of JZL184 on prostaglandin levels in mouse brain. (h-j) Effects of JZL184 on PG-G levels in mouse brain, relative to vehicle-treated mice. Each point (circle) represents a biological replicate (one mouse). Veh n=10, JZL184 n=9. Error bars represent S.E.M. * p<0.05, **p<0.01, ***p<0.001, ****p<0.0001 by t-test.

1
2
3 To determine whether PG-Gs are present in mouse brain, we extracted lipids from one
4 hemisphere of C57/Bl6J mouse brains and analyzed them for PG-G levels. Under these
5 conditions, we were unable to detect any native PG-G species, consistent with our previous
6 attempts and previously published studies^{20, 24} (Fig. 1h-j, vehicle-treated mice). We hypothesized
7 that COX-2-mediated generation of PG-Gs might be substrate-limited, and thus the lack of
8 detectable PG-Gs may be due to insufficient levels of 2-AG available for oxygenation by COX-
9 2. To test this hypothesis, we administered the MAGL inhibitor JZL184 (40 mg/kg) to elevate 2-
10 AG levels. As expected, 2-AG levels were significantly elevated after JZL184 treatment,
11 whereas free AA levels were reduced, and AEA levels were unchanged (Fig. 1b-d). Also,
12 consistent with previous studies, levels of PGs were reduced in JZL184-treated mice relative to
13 vehicle-treated mice¹⁵ (Fig. 1e-g). Despite elevated 2-AG levels present in the brains of JZL184-
14 treated mice, we were still unable to detect PG-Gs under these conditions (Fig. 1h-j). It has been
15 suggested that PG-Gs are metabolized by MAGL²⁶, therefore the lack of detectable PG-Gs after
16 JZL184 treatment was quite surprising and suggests that elevation of 2-AG combined with PG-G
17 degradation inhibition may not be sufficient for generation of detectable levels of PG-Gs.
18 Alternatively, the levels of 2-AG may not be sufficiently high after JZL184 treatment to allow
19 for PG-G formation.
20
21
22
23
24
25
26
27
28
29
30
31
32
33
34
35
36
37
38
39
40
41

42 We next considered the possibility that COX-2 levels are too low to generate detectable
43 levels of PG-Gs under basal conditions. To test this hypothesis, we utilized COX-2-Tg mice that
44 overexpress human COX-2 (hCOX-2) in neurons. COX-2-Tg mice showed high levels of
45 hCOX-2 in the cerebellum and prefrontal cortex (PFC) consistent with previous studies²⁷ (Fig.
46 2a). Levels of PGs, but not free AA, were highly elevated in COX-2-Tg mice (Fig. 2b-c),
47 however we were unable to detect PG-Gs in vehicle-treated COX-2-Tg mice (Fig 2d-f). In
48
49
50
51
52
53
54
55
56
57
58
59
60

contrast, when COX-2-Tg mice were treated with JZL184, a variety of PG-Gs were easily detected (Fig. 2d-f).

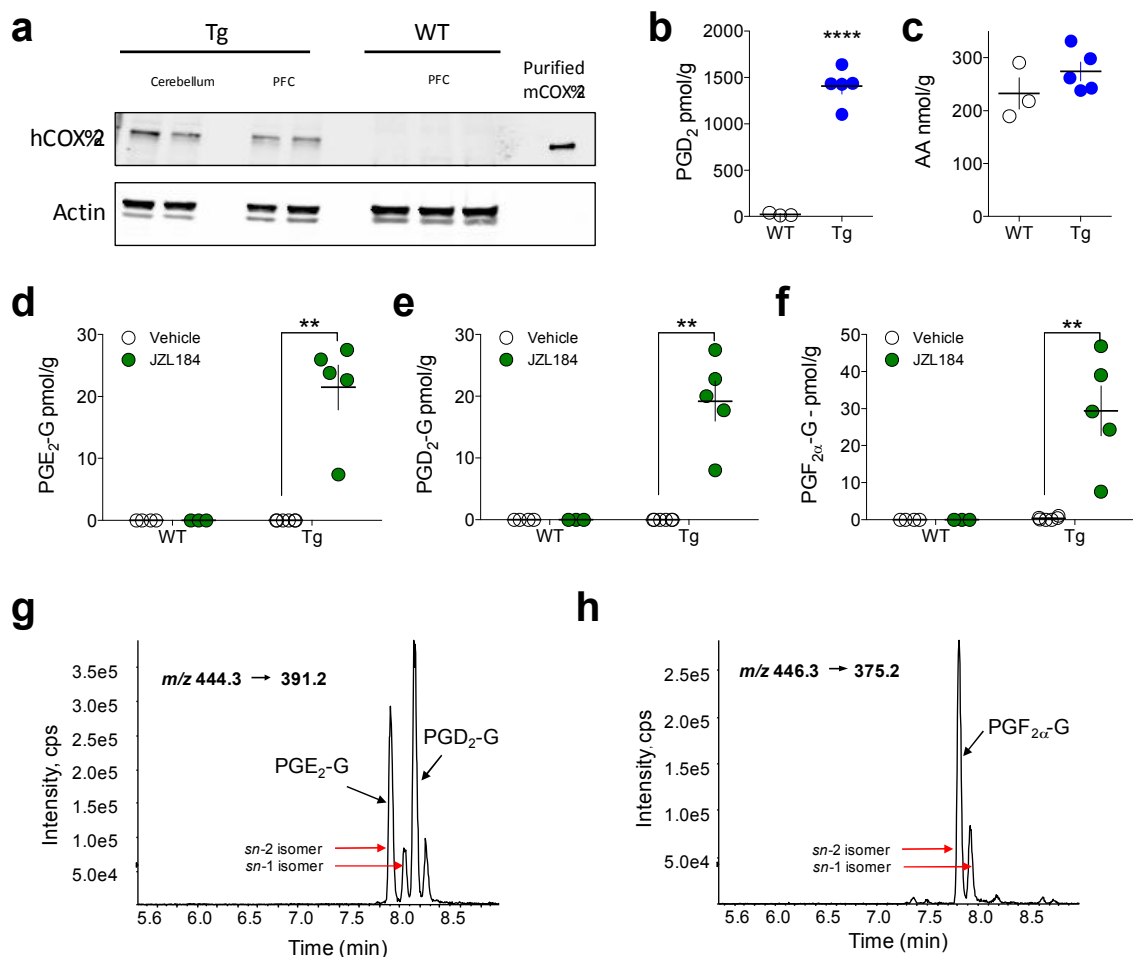


Figure 2. Detection of PG-Gs in COX-2-Tg mice after MAGL inhibition. (a) Validation of COX-2 overexpression in COX-2-Tg mice by western blot. (b-c) COX-2-Tg mice (Tg; n=5, WT; n=3) exhibit high levels of PGD₂ but not AA. (d-f) Effects of JZL184 on PG-G levels in WT and COX-2-Tg mice (WT Veh n=4, WT JZL n=3, Tg Veh n=6, Tg JZL n=5). (g-h) Representative chromatograms of endogenous PGE₂-G, PGD₂-G, and PGF_{2α}-G in COX-2-Tg mouse brain after JZL184 treatment. ** p<0.01, **** p<0.0001 by t-test (b) or Holm-Sidak test after two-way ANOVA (d-f). Each point (circle) represents a biological replicate (one mouse). Error bars represent S.E.M. Also see Supplementary Fig. 2 (c-d) for representative chromatogram of native PG-Gs using alternate SRM transitions.

Specifically, we detected both *sn*-1 and *sn*-2 isomers of PGE₂-G, PGD₂-G and PGF_{2α}-G in the brains of COX-2-Tg mice treated with JZL184 (40 mg/kg) (Fig. 2d-f and g-h). The *sn*-2 isomer

predominated in all cases (Fig. 2g-h and Fig. S2c-d for confirmatory analysis using alternate SRM transitions). Detection of PG-Gs in COX-2-Tg mice was not due to higher levels of 2-AG after JZL184 treatment relative to WT mice, as 2-AG levels were comparable in WT and COX-2-Tg mice after JZL184 treatment (Fig. S3).

In order to confirm the increase in PG-Gs observed in COX-2-Tg mice after JZL184 treatment was indeed mediated via enzymatic activity of COX-2, we pretreated COX-2-Tg mice with the highly selective COX-2 inhibitor lumiracoxib (LMX; 5 mg/kg). LMX treatment resulted in high drug levels in brain tissue (Fig. 3a) and prevented formation of PG-Gs in COX-2-Tg mice treated with JZL184 (Fig 3b-d). LMX also reduced PG levels in COX-2-Tg mice treated with JZL184 (Fig. 3e-h).

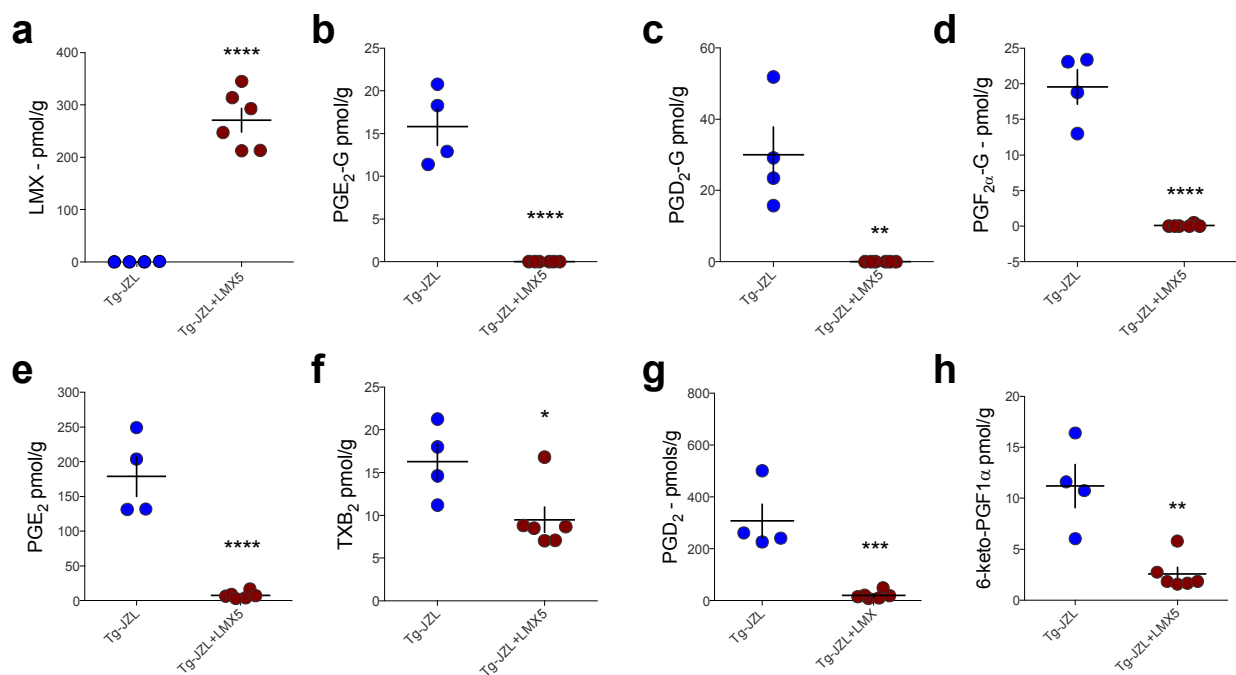


Figure 3. Lumiracoxib (LMX) reduces PG-G levels in COX-2-Tg mice treated with JZL184. (a) LMX is detected at high levels in brain after i.p. administration (5 mg/kg). (b-d) LMX treatment reduced PG-G levels in JZL184-treated COX-2-Tg mice. (e-h) LMX decreased PG levels in JZL184-treated COX-2-Tg mice (Tg-JZL n=4, Tg-JZL+LMX n=6). * p<0.05, ** p<0.01, *** p<0.001, ****p<0.0001 by unpaired t-test. Each point (circle) represents a biological replicate (one mouse). Error bars represent S.E.M.

1
2
3 We also investigated the effects of two putative substrate-selective COX-2 inhibitors, *R*-
4 flurbiprofen²⁸ (9 mg/kg) and LM-4131²⁹ (10 mg/kg), in combination with JZL184 (40
5 mg/kg) in COX-2-Tg mice. Both *R*-flurbiprofen and LM-4131 prevented the formation of PG-
6 Gs, and also reduced levels of all PG species, in COX-2-Tg mice treated with JZL184 (Fig.
7 S4). These data suggest that under the conditions used here, neither compound demonstrated
8 clear substrate-selective profile *in vivo*. However, we found that ~10% of LM-4131 converted to
9 indomethacin, and also detected *S*-flurbiprofen in *R*-flurbiprofen-treated mice (Fig. S5),
10 suggesting pharmacokinetic issues could complicate interpretation of these findings since neither
11 indomethacin² nor *S*-flurbiprofen are substrate-selective.
12
13
14
15
16
17
18
19
20
21
22
23

24 Lastly, the detection of PG-Gs have been reported in other *in vivo* models of increased
25 COX-2 expression, namely under inflammatory conditions³⁰. To assess the potential COX-2-
26 mediated generation of PG-Gs using an inflammatory model of increased COX-2 expression, we
27 induced neuroinflammation in mice using lipopolysaccharide (LPS) treatment. We pretreated
28 WT mice with LPS (3 mg/kg, once daily for two days), and JZL184 2h prior to sacrifice. LPS
29 alone and LPS combined with JZL184 increased PGE₂ and 6-keto-PGF_{1α} (Fig. 4 a-d) while only
30 LPS combined with JZL184 significantly increased PG-G levels (Fig. 4 e-f), albeit to levels
31 approximately 100-fold lower than seen in COX-2-Tg mice treated with JZL184.
32
33
34
35
36
37
38
39
40
41
42
43
44
45
46
47
48
49
50
51
52
53
54
55
56
57
58
59
60

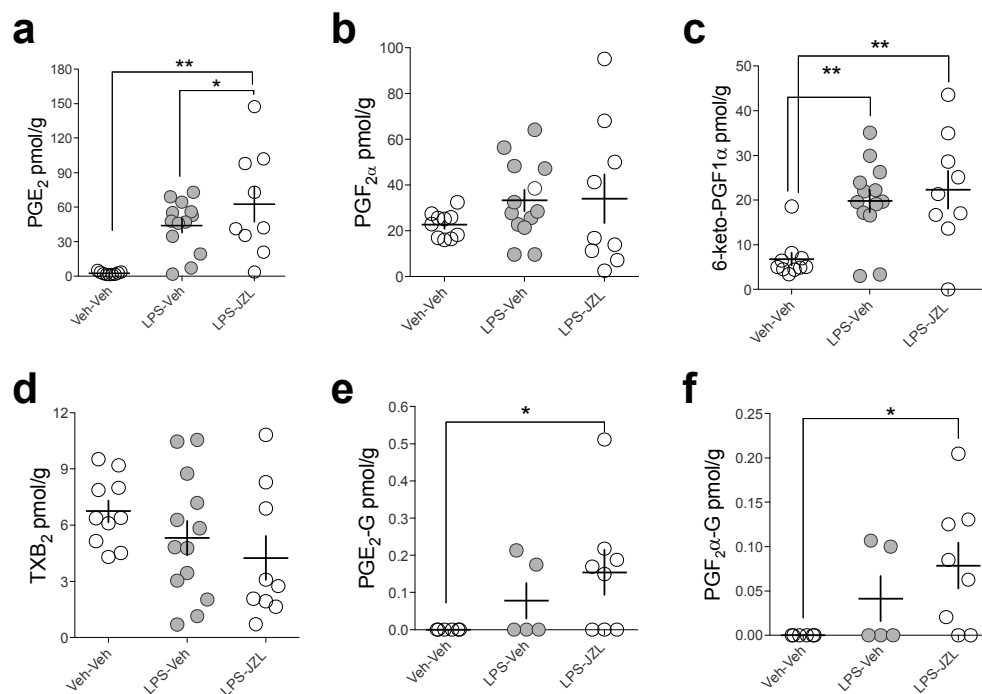


Figure 4. LPS combined with JZL184 pretreatment increases PG and PG-G levels in brain. (a-d) LPS (3 mg/kg, twice over 48 hours) and LPS+JZL increased PGE₂ and 6-keto-PGF_{1α} levels in WT mice (Veh-Veh n=10, LPS-Veh n=13, LPS-JZL n=9). (e-f) LPS+Veh and LPS+JZL did not significantly increase PG-Gs in WT mice (Veh-Veh n=6, LPS-Veh n=5, LPS-JZL n=8). * p<0.05, ** p<0.01 by Fisher's LSD test after one-way ANOVA. Each point represents biological replicate (one mouse). Error bars represent S.E.M.

Here we show that PG-Gs are generated in mouse brain under conditions of increased neuronal COX-2 expression combined with elevated 2-AG levels. Given that our approach to elevating 2-AG utilized inhibition of MAGL, which has also been suggested to hydrolyze PG-Gs²⁶, it is likely that PG-G hydrolysis inhibition facilitated *in vivo* detection of PG-Gs under these conditions. This is in contrast to prostamides, which are not hydrolyzed by FAAH¹³, which may account for their previous *in vivo* detection^{11, 12}. Our data also indicate a requirement for COX-2 enzymatic activity in the generation of PG-Gs, since formation was prevented by the highly selective COX-2 inhibitor LMX. In addition to LMX, we utilized two other compounds that have demonstrated substrate-selective activity (i.e. preferentially inhibiting 2-AG

1
2
3 oxygenation by COX-2 over AA) in various assays, *R*-flurbiprofen²⁸ and LM-4131²⁹. Both
4
5 compounds prevented the formation of most PGs and PG-Gs to a similar degree indicating a lack
6
7 of substrate-selectivity *in vivo*. Our data indicate that *in vitro* substrate-selectivity of these
8
9 compounds does not translate to *in vivo* substrate-selectivity, possibly due to *in vivo* conversion
10
11 to non-substrate-selective metabolites. Development of metabolically stable substrate-selective
12
13 probes is needed to determine whether substrate-selectivity measured in recombinant enzymatic
14
15 and cellular assays can be measured *in vivo*.
16
17
18

19 The function of PG-G signaling is not well understood. At the synaptic level, exogenous
20
21 PG-Gs can increase inhibitory neurotransmission, possibly via release of intracellular calcium¹⁶;
22
23 these effects are opposite those seen with 2-AG which *decreases* inhibitory neurotransmission
24
25 via CB1 receptor activation^{6, 16}. Therefore, it is possible that elevated neuronal COX-2
26
27 expression represents a mechanism by which traditional eCB signaling can be “switched” from
28
29 inhibition to facilitation of presynaptic neurotransmitter release through generation of PG-Gs
30
31 acting through an as of yet unidentified receptor target. Interestingly, the recent report that PG-
32
33 Gs activate P2Y6 receptors²⁵, which are known to trigger calcium release in astrocytes³¹,
34
35 suggests that PG-Gs may indirectly regulate neurotransmission via astrocyte-neuronal crosstalk.
36
37 Based on our findings, the conditions under which PG-G signaling occurs would most likely
38
39 require elevated COX-2 expression and increased levels of 2-AG production, such as those
40
41 observed after brain injury or inflammation for example³²⁻³⁶. That LPS injection combined with
42
43 JZL184 treatment led to the detection of PG-Gs (albeit at very low levels) further supports this
44
45 notion. Future studies should be aimed at determining the precise physiological or
46
47 pathophysiological conditions under which PG-Gs are generated and the functional significance
48
49 of these signaling molecules.
50
51
52
53
54
55
56
57
58
59
60

Methods

Animals: Male and female COX-2-Tg mice (Jackson Laboratories, Bar Harbor, ME; JAX stock #010703) that overexpress COX-2 under the neuron specific Thy-1 promoter or wild-type littermates derived from heterozygous breeding pairs were used as subjects. Mice were 60-90 days of age at time of experimentation. COX-2-Tg and wild-type (WT) progeny were genotyped using PCR analysis of tail genomic DNA. Briefly, tail tissue from tail snips were placed on 95°C heat block in lysis solution for one hour with neutralizing solution applied immediately after. Samples were centrifuged at 4000 rpm for 3 min at 4°C. 2µl of each sample was loaded, with REDTaq DNA polymerase (Sigma-Aldrich, St. Louis, MO), autoclaved H₂O, and hCOX-2 DNA primers. Following PCR, the results were visualized with gel electrophoresis, using an agarose gel run at 105 V, 3.00 A, for 45 min. Transgenic bands were defined with a top band at 500 kb, and WT mice had top band as well as bottom band (700 kb)²⁷. All WT mice referenced in these experiments are native WT littermates of the COX-2-Tg colony. All experiments were carried out in accordance with the National Institutes of Health Guide for the Care and Use of Laboratory Animals and approved by the Vanderbilt University Office of Animal Welfare.

Drugs: The MAGL inhibitor JZL184 (40 mg/kg) and *R*-flurbiprofen (9 mg/kg) were purchased from Cayman Chemicals, Ann Arbor, MI; Lumiracoxib (5 mg/kg) from Selleck Chemicals, TX, USA; and LM-4131 (10 mg/kg), was synthesized as previously described²⁹; and were administered via intraperitoneal injection (1 ml/kg DMSO) 3 h before sacrifice. LPS (Sigma-Aldrich, St. Louis, MO), was administered via intraperitoneal injection (10 ml/kg; pyrogen-free saline), with two injections of LPS given, 24 h apart. Four hours after the second injection, mice

1
2
3 were treated with JZL184 (40 mg/kg). Mice were sacrificed 3 hours after JZL184 or DMSO
4
5 injection.
6
7
8
9

10 *Western Blot:* Western blot analysis for COX-2 was performed as previously described using a
11
12 rabbit-anti hCOX-2 antibody²⁸ (Cayman Chemicals, Ann Arbor, MI).
13
14

15
16
17 *LC-MS/MS:* Whole mouse brains were frozen on dry ice and stored at -80°C prior to processing and
18
19 analysis. Brain tissue was prepared for LC-MS/MS analysis as previously described. All LC-MS/MS
20
21 analysis was performed on a Shimadzu Nexera system in-line with a SCIEX 6500 QTrap as
22
23 previously described³⁷. The QTrap was equipped with a TurboV Ionspray source and operated
24
25 in both positive and negative ion mode. SCIEX Analyst software (ver 1.6.2) was used to control
26
27 the instruments and acquire and process the data. The deuterated internal standards AEA-d4, 2-
28
29 AG-d5, AA-d8, PGE₂-d4, PGD₂-d4, PGF_{2α}-d4, 6-keto-PGF_{2α}-d4, TXB₂-d4, PGE₂-G-d5 were
30
31 purchased from Cayman Chemicals (Ann Arbor, MI). Authentic unlabeled standards of these
32
33 analytes also were purchased from Cayman.
34
35
36
37

38 For PG, eCB, and AA analysis, the analytes were chromatographed on an Acquity UPLC
39
40 BEH C18 reversedphase- column (5.0 x 0.21 cm; 1.7 μm) which was held at 40°C. A gradient
41
42 elution profile was applied to each sample; %B was increased from 15% (initial conditions) to
43
44 99% over 4.0 min and held at 99% for another minute. Then the column was returned to initial
45
46 conditions for 1.5 min prior to the next injection. The flow rate was 330 μL/min and component
47
48 A was water with 0.1% formic acid while component B was 2:1 acetonitrile:methanol (v/v) with
49
50 0.1% formic acid.
51
52
53
54
55
56
57
58
59
60

1
2
3 For PG-G analysis, the analytes were chromatographed on a Acquity BEH C18 column
4 (10.0 x 0.21 cm; 1.7 μm) which was held at 42°C. A gradient elution profile was applied to each
5 sample; %B was increased from 6% (initial conditions) to 50% over 8.5 min, then increased to
6 99% over 0.5 min and held at 99% for another 2.2 min. Finally, the column was returned to
7 initial conditions for 2.5 min prior to the next injection. The flow rate was 300 $\mu\text{L}/\text{min}$ and
8 component A was 10 mM ammonium acetate (pH adjusted to approximately ≈ 3.3 with glacial
9 acetic acid) while component B was acetonitrile with 5% component A.
10
11
12
13
14
15
16
17
18

19 All analytes were detected using a SCIEX 6500 QTrap via selected reaction monitoring.
20 Table S1 gives the Q1 and Q3 m/z values, collision energy (CE), declustering potential (DP) and
21 ionization mode for all analytes and their respective internal standards. Analytes were
22 quantitated by stable isotope dilution against their deuterated internal standard. Data was
23
24
25
26
27
28
29
30
31
32
33
34
35
36
37
38
39
40
41
42
43
44
45
46
47
48
49
50
51
52
53
54
55
56
57
58
59
60

normalized to tissue mass and are presented as either “pmol/g tissue” or “nmol/g tissue”.

Abbreviations

Collision energy (CE), collision-induced dissociation (CID), cyclooxygenase-2 (COX-2), declustering potential (DP), endogenous cannabinoid (eCB), liquid chromatography- tandem mass spectrometry (LC-MS/MS), mass to charge ratio (m/z), monoacylglycerol lipase (MAGL), prefrontal cortex (PFC), prostaglandin glyceryl esters (PG-G), prostaglandin ethanolamide (PG-EA), selected reaction monitoring (SRM), transgenic (Tg), 2-arachidonoylglycerol (2-AG), anandamide (AEA), fatty-acid amide hydrolase (FAAH), arachidonic acid (AA), lipopolysaccharide (LPS), lumiracoxib (LMX).

Author Information

Author contributions: A.M. generated and genotyped mice, performed *in vivo* experiments, and prepared tissue for analysis; P.J.K. performed LC-MS/MS analytical analysis; and M.M.M. performed western blot experiments under supervision of S.P. and L.J.M. M.A., T.P., and A.G., contributed to mouse model generation, tissue preparation, and genotyping under supervision of S.P. A.M. and S.P. wrote the manuscript with input from all authors.

Funding Sources: This work was supported by NIH Grants MH100096 (S.P) and S10OD017997. A.M. was supported by T32MH065215.

Conflicts of Interest: Vanderbilt University owns patent #14/415,977 entitled “Compositions and Methods for Substrate-Selective Inhibition of Endocannabinoid Oxygenation.” S.P. is a scientific consultant for Psy Therapeutics and has an active research contract with H. Lundbeck A/S.

Supporting Information

Table S1. Mass Spectral Parameters for Lipid Analysis

Figure S1. Isomerization of PG-Gs.

Figure S2. PGE₂-G and PGD₂-G Chromatography.

Figure S3. 2-AG levels in WT and COX-2-Tg mice.

Figure S4. *R*-flurbiprofen and LM-4131 reduce PG-G levels in COX-2-Tg mice treated with JZL184.

Figure S5. *In vivo* metabolism of LM-4131 and *R*-flurbiprofen.

- 1 Prospero-Garcia, O., Amancio-Belmont, O., Becerril Melendez, A. L., Ruiz-Contreras, A. E., and Mendez-Diaz, M. (2016) Endocannabinoids and sleep, *Neurosci Biobehav Rev* 71, 671-679.
- 2
- 3
- 4
- 5
- 6
- 7
- 8
- 9
- 10
- 11
- 12
- 13
- 14
- 15
- 16
- 17
- 18
- 19
- 20
- 21
- 22
- 23
- 24
- 25
- 26
- 27
- 28
- 29
- 30
- 31
- 32
- 33
- 34
- 35
- 36
- 37
- 38
- 39
- 40
- 41
- 42
- 43
- 44
- 45
- 46
- 47
- 48
- 49
- 50
- 51
- 52
- 53
- 54
- 55
- 56
- 57
- 58
- 59
- 60

17. Kozak, K. R., Rowlinson, S. W., and Marnett, L. J. (2000) Oxygenation of the endocannabinoid, 2-arachidonoylglycerol, to glyceryl prostaglandins by cyclooxygenase-2, *J Biol Chem* 275, 33744-33749.
18. Straiker, A., Wager-Miller, J., Hu, S. S., Blankman, J. L., Cravatt, B. F., and Mackie, K. (2011) COX-2 and fatty acid amide hydrolase can regulate the time course of depolarization-induced suppression of excitation, *Br J Pharmacol* 164, 1672-1683.
19. Kim, J., and Alger, B. E. (2004) Inhibition of cyclooxygenase-2 potentiates retrograde endocannabinoid effects in hippocampus, *Nat Neurosci* 7, 697-698.
20. Chicca, A., Gachet, M. S., Petrucci, V., Schuehly, W., Charles, R. P., and Gertsch, J. (2015) 4'-O-methylhonokiol increases levels of 2-arachidonoyl glycerol in mouse brain via selective inhibition of its COX-2-mediated oxygenation, *J Neuroinflammation* 12, 89.
21. Rouzer, C. A., and Marnett, L. J. (2005) Glycerylprostaglandin synthesis by resident peritoneal macrophages in response to a zymosan stimulus, *J Biol Chem* 280, 26690-26700.
22. Rouzer, C. A., Tranguch, S., Wang, H., Zhang, H., Dey, S. K., and Marnett, L. J. (2006) Zymosan-induced glycerylprostaglandin and prostaglandin synthesis in resident peritoneal macrophages: roles of cyclo-oxygenase-1 and -2, *Biochem J* 399, 91-99.
23. Alhouayek, M., Masquelier, J., Cani, P. D., Lambert, D. M., and Muccioli, G. G. (2013) Implication of the anti-inflammatory bioactive lipid prostaglandin D2-glycerol ester in the control of macrophage activation and inflammation by ABHD6, *Proc Natl Acad Sci U S A* 110, 17558-17563.
24. Hu, S. S., Bradshaw, H. B., Chen, J. S., Tan, B., and Walker, J. M. (2008) Prostaglandin E2 glycerol ester, an endogenous COX-2 metabolite of 2-arachidonoylglycerol, induces hyperalgesia and modulates NFkappaB activity, *Br J Pharmacol* 153, 1538-1549.
25. Bruser, A., Zimmermann, A., Crews, B. C., Sliwoski, G., Meiler, J., Konig, G. M., Kostenis, E., Lede, V., Marnett, L. J., and Schoneberg, T. (2017) Prostaglandin E2 glyceryl ester is an endogenous agonist of the nucleotide receptor P2Y6, *Sci Rep* 7, 2380.
26. Savinainen, J. R., Kansanen, E., Pansar, T., Navia-Paldanius, D., Parkkari, T., Lehtonen, M., Laitinen, T., Nevalainen, T., Poso, A., Levonen, A. L., and Laitinen, J. T. (2014) Robust hydrolysis of prostaglandin glycerol esters by human monoacylglycerol lipase (MAGL), *Mol Pharmacol* 86, 522-535.
27. Vidensky, S., Zhang, Y., hand, T., Goellner, J., Shaffer, A., Isakson, P., and Andreasson, K. (2003) Neuronal overexpression of COX-2 results in dominant production of PGE2 and altered fever response, *Neuromolecular Med* 3, 15-28.
28. Duggan, K. C., Hermanson, D. J., Musee, J., Prusakiewicz, J. J., Scheib, J. L., Carter, B. D., Banerjee, S., Oates, J. A., and Marnett, L. J. (2011) (R)-Profens are substrate-selective inhibitors of endocannabinoid oxygenation by COX-2, *Nat Chem Biol* 7, 803-809.
29. Hermanson, D. J., Hartley, N. D., Gamble-George, J., Brown, N., Shonesy, B. C., Kingsley, P. J., Colbran, R. J., Reese, J., Marnett, L. J., and Patel, S. (2013) Substrate-selective COX-2 inhibition decreases anxiety via endocannabinoid activation, *Nat Neurosci* 16, 1291-1298.
30. Alhouayek, M., and Muccioli, G. G. (2014) COX-2-derived endocannabinoid metabolites as novel inflammatory mediators, *Trends Pharmacol Sci* 35, 284-292.
31. Fischer, W., Appelt, K., Grohmann, M., Franke, H., Norenberg, W., and Illes, P. (2009) Increase of intracellular Ca²⁺ by P2X and P2Y receptor-subtypes in cultured cortical astroglia of the rat, *Neuroscience* 160, 767-783.

- 1
2
3 32. Panikashvili, D., Simeonidou, C., Ben-Shabat, S., Hanus, L., Breuer, A., Mechoulam, R., and
4 Shohami, E. (2001) An endogenous cannabinoid (2-AG) is neuroprotective after brain injury,
5 *Nature* 413, 527-531.
6
7 33. Hartig, W., Michalski, D., Seeger, G., Voigt, C., Donat, C. K., Dulin, J., Kacza, J.,
8 Meixensberger, J., Arendt, T., and Schuhmann, M. U. (2013) Impact of 5-lipoxygenase
9 inhibitors on the spatiotemporal distribution of inflammatory cells and neuronal COX-2
10 expression following experimental traumatic brain injury in rats, *Brain Res* 1498, 69-84.
11 34. Gunther, M., Plantman, S., Davidsson, J., Angeria, M., Mathiesen, T., and Risling, M. (2015)
12 COX-2 regulation and TUNEL-positive cell death differ between genders in the secondary
13 inflammatory response following experimental penetrating focal brain injury in rats, *Acta*
14 *Neurochir (Wien)* 157, 649-659.
15 35. Minghetti, L. (2004) Cyclooxygenase-2 (COX-2) in inflammatory and degenerative brain
16 diseases, *J Neuropathol Exp Neurol* 63, 901-910.
17 36. Tzeng, S. F., Hsiao, H. Y., and Mak, O. T. (2005) Prostaglandins and cyclooxygenases in
18 glial cells during brain inflammation, *Curr Drug Targets Inflamm Allergy* 4, 335-340.
19 37. Bedse, G., Hartley, N. D., Neale, E., Gaulden, A. D., Patrick, T. A., Kingsley, P. J., Uddin,
20 M. J., Plath, N., Marnett, L. J., and Patel, S. (2017) Functional Redundancy Between Canonical
21 Endocannabinoid Signaling Systems in the Modulation of Anxiety, *Biol Psychiatry* 82, 488-499.
22
23
24
25
26
27
28
29
30
31
32
33
34
35
36
37
38
39
40
41
42
43
44
45
46
47
48
49
50
51
52
53
54
55
56
57
58
59
60

